IOSR Journal of Mechanical and Civil Engineering (IOSR-JMCE)
e-ISSN: 2278-1684,p-ISSN: 2320-334X, Volume 15, Issue 6 Ver. III (Nov. - Dec. 2018), PP 31-43
www.iosrjournals.org

Finite Element Modelling of Structures Subjected to Thermal Loading

Hisham A. El-Arabaty[1], Gamal H. Mahmoud[2], Nasr E. Nasr[3], Mohamed A. Abdul Rahim[4]

[1] *(Structural Engineering Department, Faculty of Engineering/ Ain-Shams University, Cairo, Egypt)*
[2] *(Structural Engineering Department, Faculty of Engineering/ Ain-Shams University, Cairo, Egypt)*
[3] *(Structural Engineering Department, Faculty of Engineering/ Ain-Shams University, Cairo, Egypt)*
[4] *(Structural Engineering Department, Faculty of Engineering/ Ain-Shams University, Cairo, Egypt)*
Corresponding Author: Hisham A. El-Arabaty

Abstract: *Thermal analysis of RC structures under the effect of uniform temperature change poses a special kind of problem, where the high axial stiffness of horizontal beam elements used in finite element analysis produces correspondingly high lateral forces, and straining actions in the supporting columns, especially the ground floor columns. This effect is most pronounced for the external columns.*

In this study, a novel proposal is made for developing an analytical approach for assessment of the effect of bending cracks along the beam length on its axial stiffness. The proposed approach is utilized for the development of a software package for the computation of the effective axial stiffness of beams, taking into consideration the resulting cracked-section strains at the top and bottom fibers of the beam sections along its length. Effect of applying varying axial force levels to the beam is studied in detail, and curves are developed showing the variation of the beam's axial stiffness with the applied axial loads. Effect of different parameters including steel reinforcement level, and span length are also taken into account. The analysis results are used to develop useful recommendations for design engineers, related to the reduction factors which can be applied to beams' axial stiffnesses in finite element models, in order to simulate the practical case of thermal effect on beams subjected to bending cracks.

Keywords: *Temperature Changes, Thermal Analysis, Finite Element Modeling, Concrete Cracking (Fracturing), Reinforced Concrete, Tensile Stress.*

Date of Submission: 21-12-2018 Date of acceptance: 05-01-2019

I. Introduction

Reinforced concrete structures are commonly exposed to thermal loads as the result of the design function of the structure, ambient conditions, heat of hydration, or exposure to fire. This research study concentrates on the uniform temperature variation, which causes an increase in the horizontal dimensions of the building stories, as compared to the underground footings which undergo no temperature change and are quite restrained, thus exhibiting no movement.

The objective of this paper is to develop models matching the actual behaviour of structures under uniform temperature change as compared to the analysis models used, for evaluation of this phenomenon.

1.1 Problem Description

The expected deformed shape of a multistory building is shown in Fig. 1, where a uniform temperature rise applied to the 3-D model developed by a designer would yield the deformations shown. As can be seen, the columns most severely affected are the ground floor columns, attached at top to a floor exhibiting expansion, and at the bottom to the foundations which do not exhibit horizontal movements.

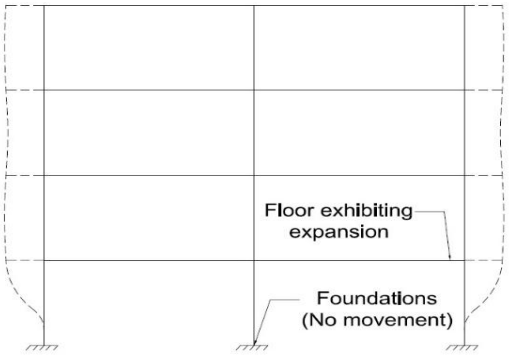

Figure1. The expected deformed shape of a multistory building under uniform temperature

The increase in length of an "Unrestrained" floor can be simply expressed as (1)

$$\Delta L = \alpha \Delta T L \quad (1)$$

Where: α is the coefficient of thermal expansion, ΔT is the change in temperature, and L is the floor length.

Analysis of common multistory buildings under the effect of thermal expansion/contraction can yield very high values for shear forces and bending moments induced into the ground floor columns by the floors expansion. Fig. 2 illustrates this phenomenon for a typical case of an RC frame. A symmetrical frame was selected for simplicity.

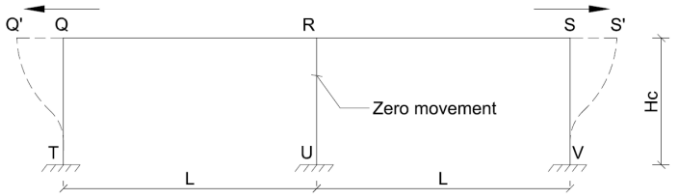

Figure2. Symmetrical RC frame

To fully grasp the magnitude of the problem, the expected unrestrained increase in beam length "ΔL" in this case will be divided into 2 components as shown in Fig. 3 below:

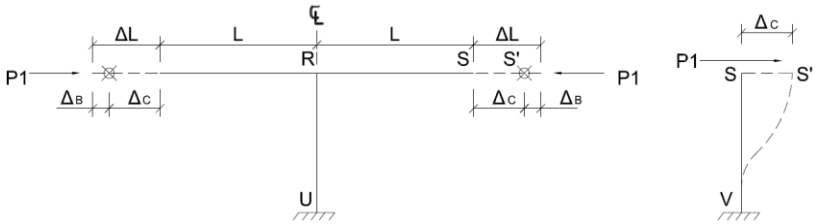

Figure 3. Influence of temperature change on structure deformation

$$\Delta L = \Delta_B + \Delta_C \quad (2)$$

Where ΔL is the unrestrained beam deformation as expressed in (1)

Δ_C is the column lateral deformation caused at the top of the edge column, and represents the actual lateral deformation of the joint considering both column & beam stiffnesses, It can be expressed as (3)

$$\Delta_C = P_1 / K_C \quad (3)$$

Where P_1 is the horizontal internal force resulting from the temperature change, and acting between the column top, and the beam edge, Kc is the transverse stiffness of the column at point S.

Δ_B is the axial deformation of one half length of the beam, and represents the difference between the unrestrained temperature deformation of the joint, and the actual final deformation, it can be expressed as (4)

$\Delta_B = P_1 / K_B$ (4)

Where K_B is the axial stiffness of half-length of the beam.
Combining (3) and (4), the total "unrestrained" expansion of the beam can be expressed as (5)

$\Delta = (P_1 / K_C) + (P_1 / K_B)$. (5)

Therefore the force P1 can be computed as (6)

$$P_1 = \Delta \left(\frac{K_B \, x \, K_C}{K_B + K_C} \right) \quad (6)$$

To summarize, the unrestrained increase in beam length "ΔL" is divided into 2 components, the first causing shear and moments on the column, and the other causing a compression force on the beam. Since the value of the beam's axial stiffness K_B is much larger than the column's bending stiffness K_C, it is to be expected that most of the deformation will go to the column, thus producing very high values of shear forces and bending moments in the columns. The same result was reached by [4]. On the other hand, an increase in the columns' sections to enhance their strength and resistance will certainly increase their stiffness, and increase the value of P_1. Thus, the designer is sometimes at a loss whether to increase the column sections to add to their capacity, or to reduce them, thus reducing the moment resulting on the column due to thermal expansion. The large value of the axial stiffness of beams and slabs is mainly responsible for the high values of straining actions in columns, obtained from analytical models used for thermal analysis of concrete skeletons under uniform temperature change. It is therefore highly important to investigate reduction factors applied to this axial stiffness of horizontal beams and slabs in analysis, and their relation to actual structural behavior.

II. Existing Literatures and Codes

In **ACI 224.2R-92 (1992) and ACI 349.1R (2007)**, two design approaches are specified for thermal analysis. The first approach depends on combining of the internal straining actions resulting from both temperature and mechanical loads, and taking into consideration the effect of concrete cracking and reinforcement yielding, thus it requires complex calculations using nonlinear finite element analysis. The second approach is an approximate approach depending on performing an elastic finite element analysis using a reduction modulus of 0.50E for concrete to take the impact of various factors, including yielding, cracking and creep. Thermal loads computed using this approach are not dependent on mechanical loads.

ECP 203 (2017) allows for the modification of the modulus of elasticity in thermal analysis, by applying a reduction factor that is not less than 0.45 to the computed value for concrete modulus of elasticity.

Essam H. El-Tayeb, Salah E. El-Metwally, Hamed S. Askar, Ahmed M. Yousef (2015) Studied the behavior of reinforced concrete elements under temperature variation with the presence of vertical loads, and found that material modeling of reinforced concrete is important for realistic behavior. Also cracking of reinforced concrete helps to release the restraint forces developed depending on the reduction in the structural stiffness.

F.J. Vecchion, Agostinoa, N D B. Angelak (1993) Tested many specimens of reinforced concrete slabs under both mechanical and thermal loads with various amounts of reinforcements. Restrained thermal deformations resulting in significant levels of cracking and stressing, thus thermal creep and cracking caused reductions in stiffness. Accordingly, rapid loss of the restraint forces developed.

Randy J. James and Ai-Shen Liu (2009) nonlinear analysis is employed for investigating the reduction in structural stiffness and resulting forces. Thermal cracking analysis results have been included in the linear-based design methods by developing an analysis procedure. Furthermore to section cracking that produce a reduction of the section forces and moments the authors found that concrete cracking reduces the structural stiffness and therefore the curb against thermal expansion or contraction of the whole structure. Stress reduction factors can be developed and used to correct the linear-based design method.

III. Analytical Algorithm

While several previous studies have investigated the effect of concrete cracking on the overall horizontal stiffness of beams and slabs, the complexity of the models used is very high, due to the incorporation of material nonlinearity, and the modeling of steel reinforcement. This makes it very difficult to perform the necessary large number of analysis runs. Moreover, the assumption that cracking in beams will occur on a level corresponding to ultimate load conditions is not realistic. In actual buildings, it is highly possible for columns to reach ultimate load levels, while the thermally induced stresses in the beams are still at a comparatively low level, within the working load limits of these beams.

For the purely theoretical case of a beam not subjected to any bending moments, a compressive force acting on the beam will produce pure compressive stresses and strains, and the following relations apply to this case:

$$\sigma = N/A \tag{7}$$

$$\varepsilon = \sigma/E \tag{8}$$

$$K_{Axial} = EA/L \tag{9}$$

However, beams and slabs in RC structures are almost always subjected to bending moments, and their sections are cracked. Within working stress limits, the beam bending behavior can be illustrated as shown in Fig. 4.

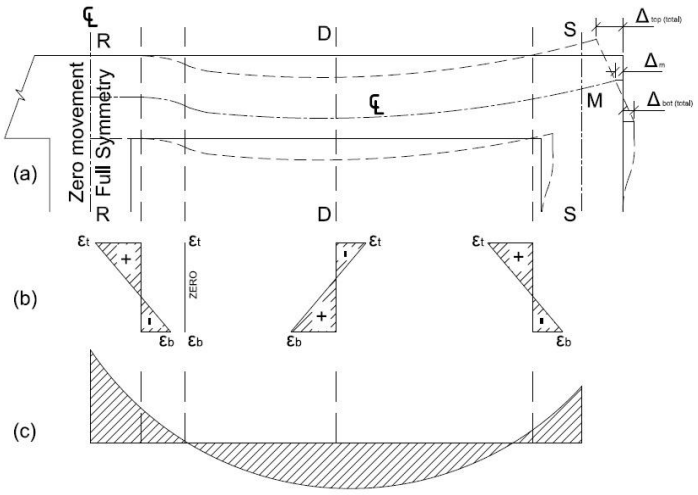

Figure 4. a) Elongation of top & bottom beam fibers due to vertical loads only b) Beam stresses at specific locations c) Beam bending moment due to vertical loads only

As shown, the different sections exhibit different stress and strain levels, depending on their location along the beam length. Fig. 5 illustrates the effect of a compressive axial force (due to partially restrained beam expansion) on a typical beam section.

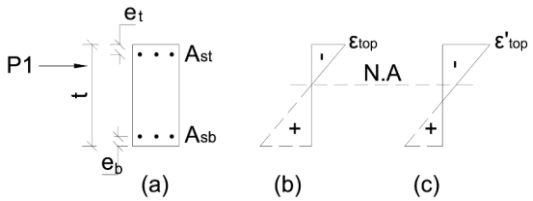

Figure 5. a) Compression force "P1" due to beam expansion b) Strain distribution in cracked section at D-D due to moment only. c) Strain distribution in cracked section at D-D due to combined effect of moment and axial force together.

As can be seen, the compressive force causes a change in the neutral axis location, and thus produces a "partial closing" effect on the cracks. The exact opposite occurs in case of a tension axial force (due to beam contraction). Due to the existence of flexure cracks in the beams, a compressive force will produce displacements through 2 mechanisms, the first involving producing compressive strains in the concrete, and the second involving "closing of flexure cracks".

The axial stiffness expression developed in (9) describes only the first mechanism (compressive strain in the concrete), and therefore cannot be applied to describe the actual behavior accurately. Consequently, it is essential to apply a reduction factor to the axial stiffness expression of (9), to simulate the actual structural behavior of the beam under compression. The same applies to axial tension forces.

In Fig. 5, the cumulative effect of the strains produced at the top and bottom fibers of the beam results in the inclination of the beam section at section S, as shown. This inclination is a direct result of an overall shortening (negative elongation) at beam top fibers, and an overall elongation (positive) at the beam bottom fibers. The resulting displacements can be expressed by (Δ_{top} and Δ_{bot}) at the top and bottom fibers of the beam at section S respectively, as shown. Using an integration approach, these displacements (produced by vertical load moments only) can be expressed as follows:

$$\Delta_{top(total)} = \int_0^L \varepsilon_{top}\, dl \tag{10}$$

$$\Delta_{bot(total)} = \int_0^L \varepsilon_{bot}\, dl \tag{11}$$

The same procedure can be used to compute the corresponding top and bottom displacements under the effect of the combined bending moment (caused by vertical loads), and axial force (caused by beam expansion/contraction), as follows:

$$\Delta'_{top(total)} = \int_0^L \varepsilon'_{top}\, dl \tag{12}$$

$$\Delta'_{bot(total)} = \int_0^L \varepsilon'_{bot}\, dl \tag{13}$$

A novel analytical approach is adopted in this study, which depends on calculation of the bending moments, and strain values developed at each section along the beam length. Dividing the beam into a large number of sections (50 to 100 divisions) allows for the calculation of these cumulative displacements using numerical integration. Using a step of Δ_s, (10) to (13) can be transformed into the following form suitable for numerical integration:

$$\Delta_{top(total)} = \sum_{n=1}^{n_{div.}} \varepsilon_{top}\, \Delta_s \tag{14}$$

$$\Delta_{bot(total)} = \sum_{n=1}^{n_{div.}} \varepsilon_{bot}\, \Delta_s \tag{15}$$

$$\Delta'_{top(total)} = \sum_{n=1}^{n_{div.}} \varepsilon'_{top}\, \Delta_s \tag{16}$$

$$\Delta'_{bot(total)} = \sum_{n=1}^{n_{div.}} \varepsilon'_{bot}\, \Delta_s \tag{17}$$

Where: Δ_s is the length of selected segment and n_{div} is the number of selected segments.
The average displacement at the midsection point "M" at section S can be calculated as the average of the top and bottom computed displacements as follows:

$$\Delta_m = \left[\Delta_{top\,(total)} + \Delta_{bot\,(total)}\right]/2 \tag{18}$$

IV. Step by Step Procedure for Computation of Beam Axial Stiffness

In this section, a step by step procedure is outlined for the implementation of the above-described analytical algorithm. The flowchart illustrated in Fig. 6 shows the layout of the step by step procedure, and can be summarized in the following steps:

1. Dividing the beam into a large number of segments "$n_{div.}$".
2. Calculating the bending moment due to vertical loads only.
3. Calculating the top and bottom fiber strains for each segment due to the bending moment only.
4. Calculating the cumulative top and bottom fiber elongation "Δ_{top} & Δ_{bot}" at the end of the beam length using (14) & (15).
5. A base-value for Δ_m is computed for the case of beam under flexure, with no axial force acting. This value of Δ_m is termed $\Delta_{m(base)}$, which is defined as the beam axial total elongation at its mid-height.
6. For different values of axial force P_{axial}, a corresponding value for Δ_m can be computed using the next three steps.
7. Apply a range of axial forces with the following values (P_{Axial_Start}, P_{Axial_End} & P_{Axial_Step}).

8. Calculating the top and bottom strains ($\boldsymbol{\varepsilon}'_{top}$ & $\boldsymbol{\varepsilon}'_{bot}$) for each segment due to both of the bending moment and the applied axial force.
9. Calculating the cumulative top and bottom fiber elongation (Δ'_{top} & Δ'_{bot}) at the end of the beam length using (14) & (15) due to both of the bending moment and the applied axial force.
10. Calculating the new axial cracked stiffness as expressed in (19) for each Δ_m.

$$K_{Axial\ (Cracked)} = \frac{P_{Axial}}{\Delta_m - \Delta_{m\ (base)}} \qquad (19)$$

11. Final results are determined.

The analytical algorithm is illustrated in Fig. 6.

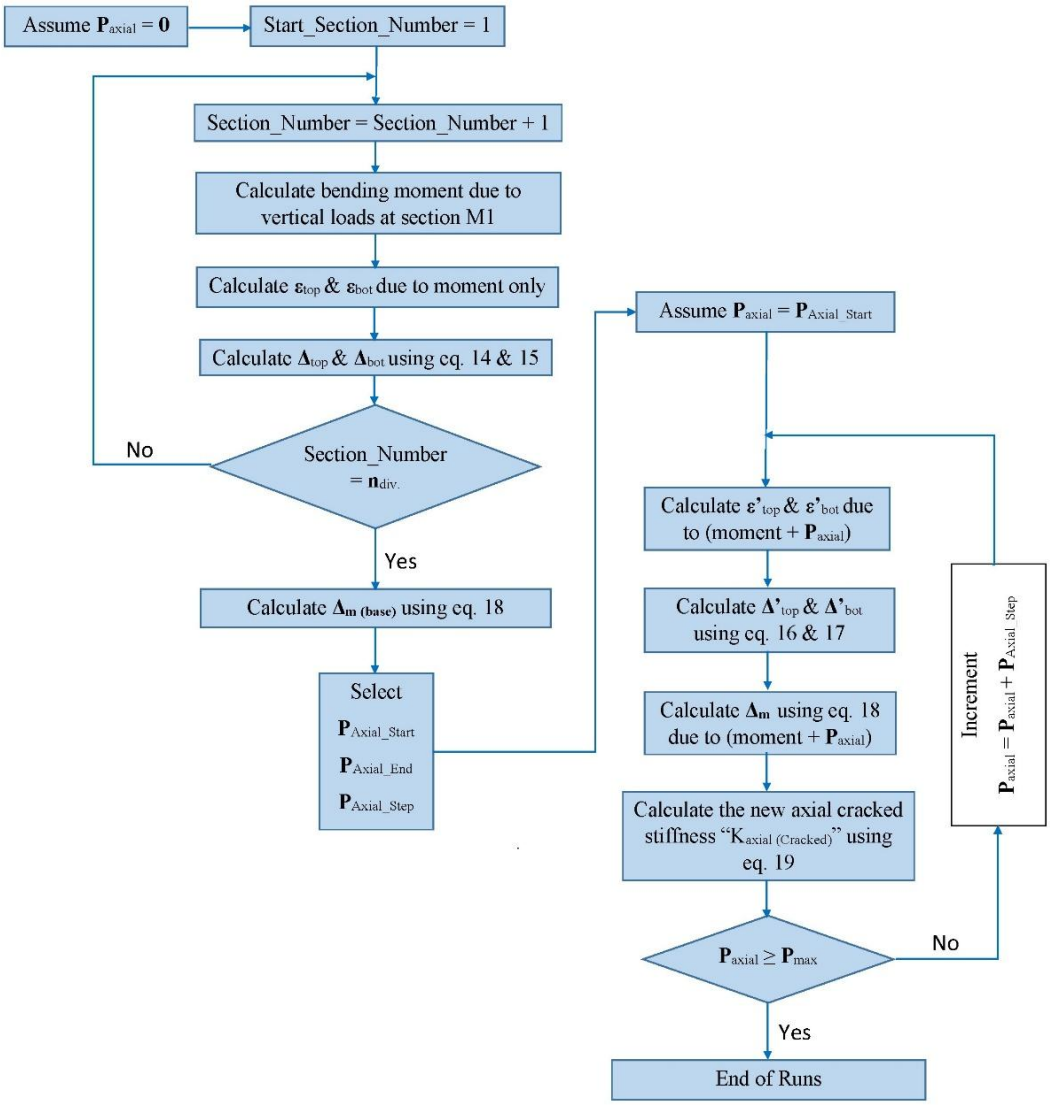

Figure 6.Analysis procedure flowchart to calculate the axial modifiers for beams' stiffness

The above-described step by step procedure is applied into a highly sophisticated software package for the structural analysis of the thermal effect of temperature change on the stiffness of horizontal structural elements.

The Visual Basic language was selected for the current package, due to its existing links to Excel sheets, and the great opportunities this provides in data input, and iterative procedures utilizing the capabilities of both the Excel program, and the Visual Basic Language.

V. Variation of Beam Stiffness with Applied Axial Load

The above-described software package is used here to determine the variation of axial stiffness of a typical beam subjected to axial forces, for both compression and tension cases. A double-span frame beam is chosen here similar to that shown in Fig. 2 & 4. Beam span is selected as 6m. Design of the beam is performed according to the Egyptian Code of Practice to carry loads corresponding to a 6m spacing between frames. Reasonable column sections are assumed, and the corresponding BMD on the beam is determined.

Based on the above-determined BMD for the beam, the developed software package is utilized to determine the crack patterns in the beam caused by the bending moments, and a detailed analysis of the 2-span beam (continuous spans of 6 m each) is performed, to determine the total axial elongation in the beam length at its CL, caused by the flexural cracks.

A wide range of axial force values is applied, while the above computed vertical load moments are applied to the beam simultaneously. Applying a series of values for the axial force acting at beam edges, (both

expansion/contraction cases), the software is used to determine the total elongation in beam CL, and consequently determine the relative displacement caused by the axial force , as compared to the "base" case of Zero axial force "$\Delta_{m(base)}$" , where bending moment effect only is acting.

The beam section used in the analysis is shown in Fig. 7, while the range of axial force variation is chosen between (-400 and +200 KN).

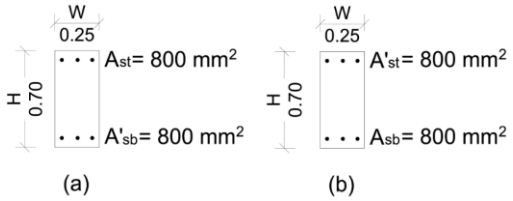

Figure 7. Beam cross-section for (case 1) at (a) "negative moment" regions (b) "positive moment" regions

The analysis results obtained from the developed software package for the above-mentioned cases are illustrated in Fig. 8.

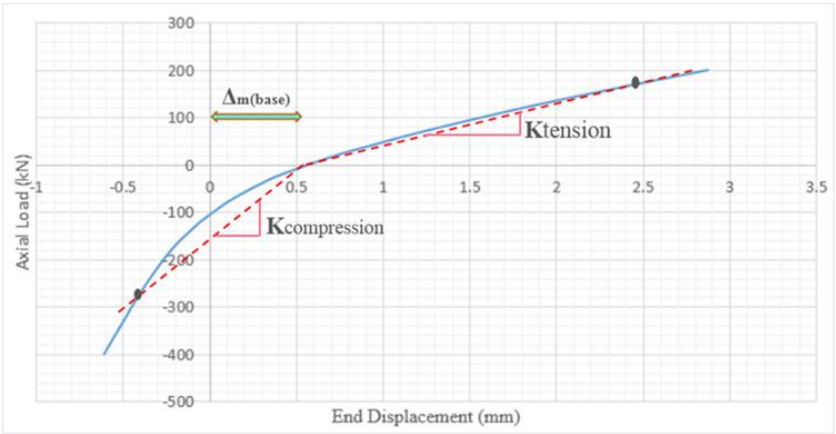

Figure 8. Force-Displacement curve for beam in axial direction

Fig. 8 illustrates the relationship between the axial load applied at the ends of the beam, and the resulting axial displacement. The positive direction of the y-axis represents tensile axial forces, while the negative direction represents compressive axial forces. The value of the beam axial stiffness at any specific axial load value can be computed using a secant approach (19).

The axial stiffness of the beam computed for both the compression and tension cases corresponds to the cases of beam expansion and contraction respectively, and can be computed as follows:

$$K_{comp} = \frac{P_{comp}}{\Delta_m - \Delta_{m\,(base)}} \quad (20)$$

$$K_{tens.} = \frac{P_{tens.}}{\Delta_m - \Delta_{m\,(base)}} \quad (21)$$

Reduction factors can be computed as follows:

$$RF_{comp} = \frac{K_{comp}}{EA/L} \tag{22}$$

$$RF_{tens.} = \frac{K_{tens.}}{EA/L} \tag{23}$$

The variation of RF_{comp} & RF_{tens} is illustrated in Fig. 9.

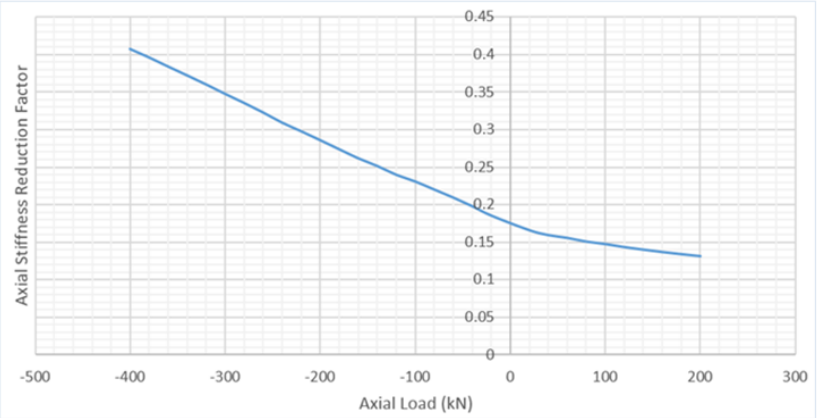

Figure 9. Force-Reduction factor curve for beam in axial direction (Case 1)

VI. Results and Discussion

Fig. 8 illustrates the structural behavior of the sample beam under axial compression and tension. For the compression case (thermal expansion), it can be seen that as the axial load increases from ZERO wthin the practical range of axial force values (0 to 400 KN), the beam stiffness increases significantly. This can be explained by the closing of cracks originally caused by the bending behavior of the loaded beams. As the cracks close more and more, the beam stiffness starts to approach the uncracked axial stiffness value. It should be noted however, that the 400 kN is a relatively high value, which is used here to cover the whole expected range. At practical values of 100 & 200 kN, the compressive axial stiffness is far less than the uncracked stiffness value, and should be considered in analysis.

On the other hand, the axial force-displacement curve in the tension zone exhibits an almost linear variation, and its change is minimal throughout the selected practical range of axial force values (0 to 200 KN). The slope of the curve (indicating the axial stiffness) is quite steep indicating a relatively low value, always less than the axial compression case, and far less than the uncracked stiffness value.

The "Axial Stiffness Reduction Factors" (RFcomp & RFtens) plotted in Fig. 9 further illustrate that the effect of beam flexural cracking on the axial stiffness of the sample beam is highly significant. For compressive forces in the practical range of 100 KN to 200 KN, the value of the reduction factor is in the range of 0.2 to 0.3 which is quite low. It reaches a maximum of 0.4 at the extreme border of the selected range at 400 KN.

For the tension case, Fig. 9 shows values of the reduction factor around the 0.15 level, reaching a maximum below 0.2 at zero tension, and plunging below 0.15 for high axial tension values. The low value of the reduction factor in this case shows the significant effect of combined bending/axial tension cracking on the expected beam axial stiffness in case of concrete contraction.

While the actual axial forces developed in typical multi-story buildings due to thermal effects vary according to the relative stiffnesses of the columns versus the beams, it can be seen that significant reduction in these axial forces is expected to occur due to the change in axial stiffness caused by flexural cracking of beams. This effect is most significant in case of low compressive axial loads, and in case of tensile axial loads.

The relative simplicity of the adopted algorithm, and the high capability of the developed software, and its short run-time has allowed for performing a wide range of analysis runs, taking into consideration a wide variety of factors. The same procedure described in section 5 was followed in the analysis of several cases of expansion/contraction of 2-span frames, to investigate the effect of different factors on the axial stiffness reduction factors.

6.1 Effect of Span Length

Different beam spans (6, 7.5 & 9 m respectively) were used. For each case, design of the beam was performed according to the Egyptian Code of Practice, and the corresponding beam sections, and steel rft amounts were input into the analysis. The data used is illustrated in Table 1.

For each case, the initial cracking of the beam section was determined according to the expected bending momens along the beam length, resulting from its analysis as a 2 bay frame. The effect of axial loads is determined at varying levels of axial forces, covering the expected practical range. Figures 10a & 10b summarize the results of analysis cases 1 to 5 as outlined in Table 1 .

Table 1. Summary of the Data Used in the Analysis

Case No.	Span Length (mm)	Section Dimensions (mm)	Steel Reinforcement Area = As (mm^2)
1	6000	250x700	800
2		250x900	750
3	7500	250x700	1250
4		250x900	1100
5	9000	250x900	1500
Case No.	Span Length (mm)	Section Dimensions (mm)	Steel Reinforcement Area = 1.3As (mm^2)
6	6000	250x700	1050
7		250x900	970
8	7500	250x700	1650
9		250x900	1450
10	9000	250x900	1970

In Fig. 10a, it can be seen that the Reduction facotrs obtained for both compression and tension axial force cases are lower for the 6m span beam than for the 7.5 m span beam. This can be directly atributed to the fact that the amount of tension steel for the 7.5 m span beam is higher based on design according to the Egyptian code of practice. This higher percentage of tension steel in all beam sections significantly increases the beam's cracked stiffness, thus producing higher reduction factors. Fig. 10b presents the same observations for a different group of cases performed on a beam with a larger section.

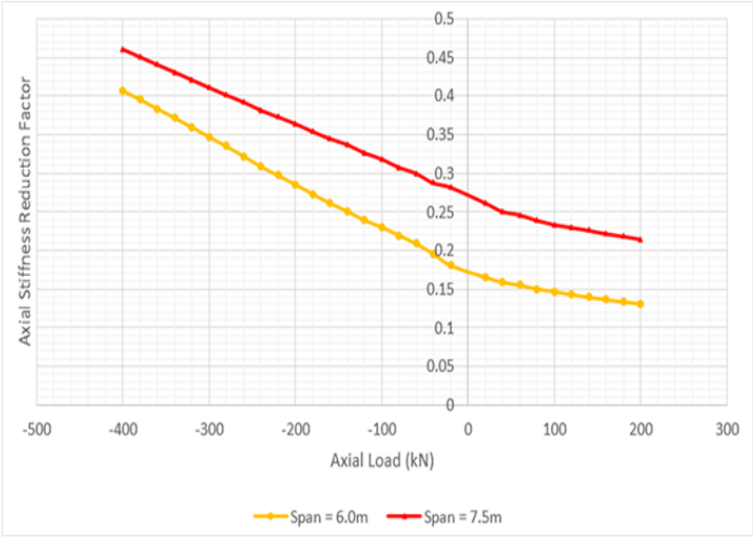

(a) Variation in axial stiffness reduction factor with beam section "25x70cm" (cases 1 & 3)

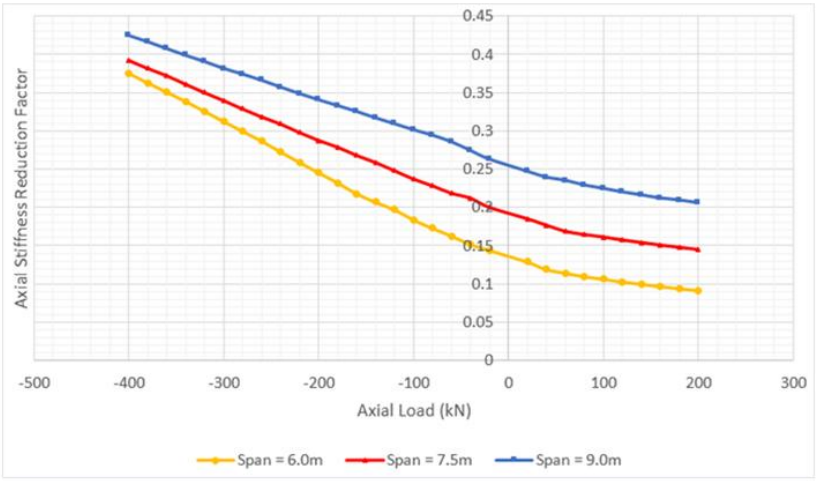

(b) Variation in axial stiffness reduction factor with beam section "25x90cm" (Cases 2 , 4 & 5)

Figure 10. Effect of span length

6.2 Effect of Section Dimensions

The effect of variation in section dimensions can be seen in Fig. 11a & 11b. It can be noted that the reduction factor curves for beams of different sections (but with the same span, and approximately the same amount of steel rft) are quite close to each other in shape, with the larger section beam showing somewhat smaller values for the reduction factor.

In order to explain the above observation, it is necessary to view it in conjunction with the results shown in Fig. 11c & 11d. As shown, the actual values of the stiffness coefficient "K" is higher for the larger section beam, in case of compressive axial loads. The observed decrease in the reduction factor is actually caused by the higher value of the "uncracked axial stiffness" of the larger beam section. As for the tensile axial loads, both curves are almost the same except for a small difference which can be explained by the smaller steel area obtained in design of the 900 mm deep beam as compared to the 700 mm deep beam.

The above observations point to an important result related to the finite element modeling of beams under thermal effect. The case of a large beam section with a relatively small rft value would produce an exaggerated "uncracked axial stiffness" to be used by a commercial software package for analysis, while the actual cracked stiffness is far less due to the small steel area. A significant reduction factor (of low value) is appropriate for this case.

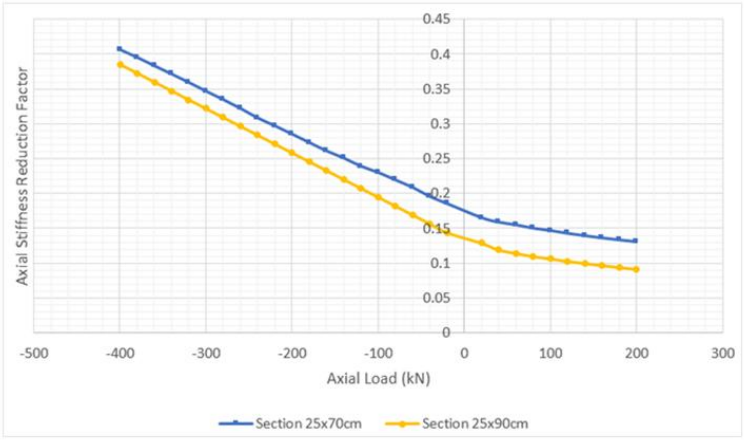

(a) Variation in axial stiffness reduction factor "Span = 6.0m" (Cases 1 & 2)

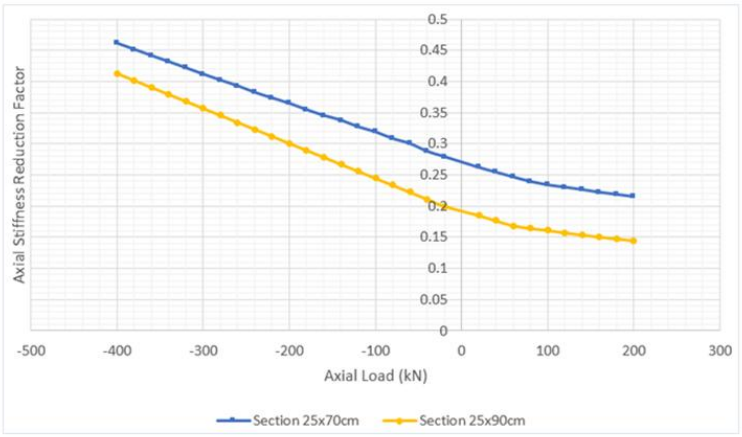

(b) Variation in axial stiffness reduction factor "Span = 7.5m" (Cases 3 & 4)

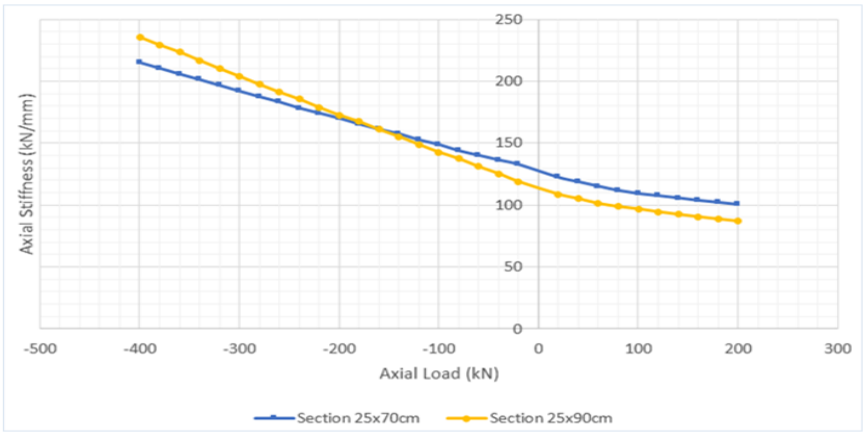

(c) Variation in axial stiffness "Span = 6.0m" (Cases 1 & 2)

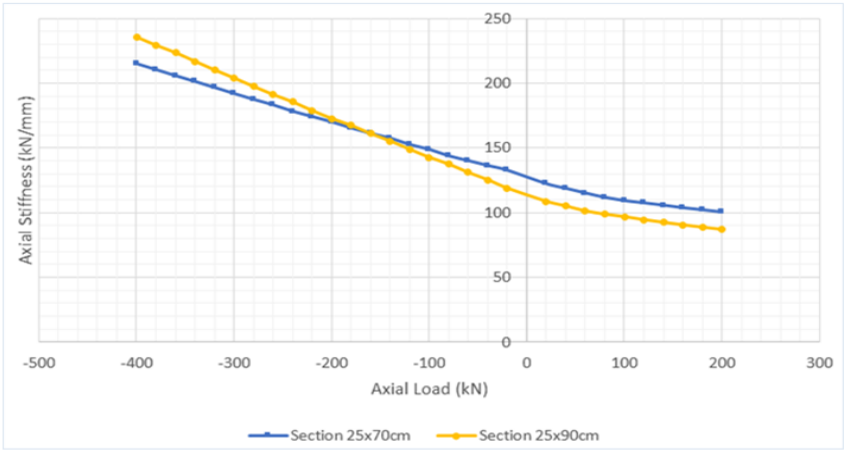

(d) Variation in Axial Stiffness "Span = 7.5m" (Cases 3 & 4)

Figure 11. Effect of section dimensions

6.3 Effect of Area of Steel Reinforcement in Section

The effect of variation in steel reinforcement area in the beam section can be seen in Fig. 12a & 12b. It can be seen clearly that increasing the amount of steel rft in the section, while fixing all other parameters has a direct effect on the "Axial Stiffness Reduction Factors".

The increase in values of the reduction factors with the increase in steel rft area produces an almost complete vertical shift for the reduction factor variation curves for both compression and tension cases. This significant effect of steel rft area on the reduction factor values indicates that the use of a fixed reduction factor

for all cases of temperature analysis is not appropriate. The values of the reduction factors to be used for analysis should be tied to the general percentage of steel rft in the beam sections.

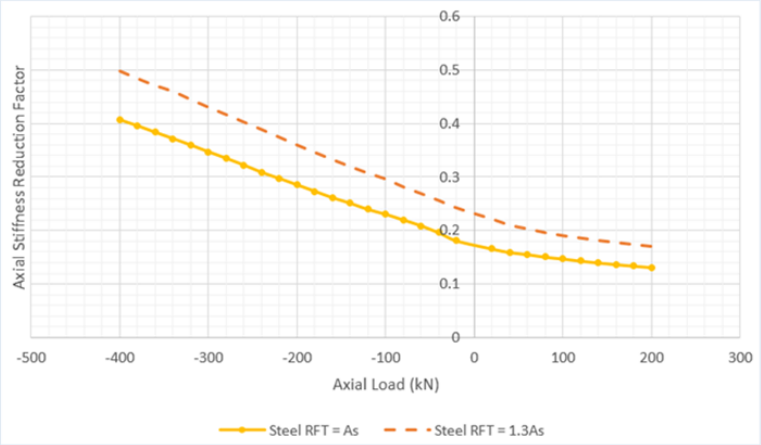

(a) Variation in axial stiffness reduction factor "Span = 6.0m" (Cases 1 & 6)

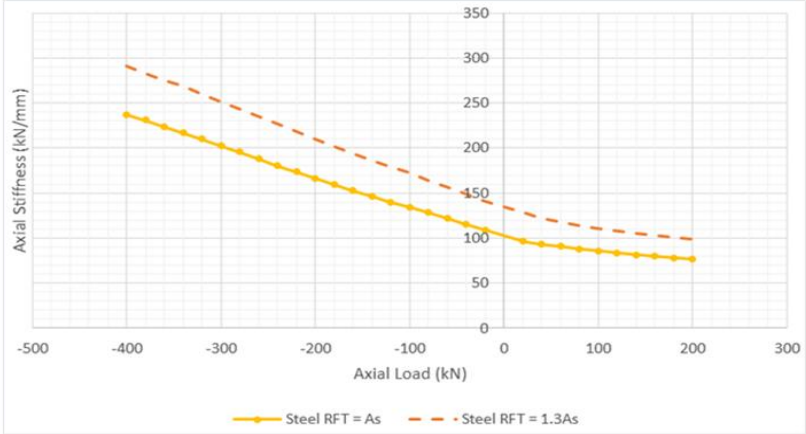

(b) Variation in axial stiffness "Span = 6.0m" (Cases 1 & 6)
Figure 12. Effect of steel reinforcement percentage in section

VII. Summary and Conclusions

In this study, the practical problem of uniform temperature effect on RC buildings is addressed, with an emphasis on the modeling of these buildings for finite element analysis under thermal loads. A new analytical approach is developed to simulate the effect of existing bending cracks along the beam length on the axial stiffness of the beam. A sophisticated software package was developed to compute the resulting beam end displacements through numerical integration of the resulting strains in the top and bottom beam fibers. The developed package is a highly useful tool for assessment of the cracking effect on beams' axial stiffness.

Analysis results obtained from the developed software, are used to compute stiffness-reduction coefficients for the cases of expansion, and contraction of a beam-column frame under the effect of varying axial forces. The obtained curves cover a complete range of realistic axial force values to which the beam can be subjected in cases of uniform expansion/contraction, and can be used in an overall analysis of a multistorey building to determine stiffness-reduction coefficients to be applied to each floor of the finite element model, depending on the level of axial force developed in the beams of each floor.

In general, analysis results showed that the stiffness reduction coefficients increased with increase of the compressive axial forces, and decreased with the increase of tensile axial forces. The effect of different parameters on these reduction factors has been studied. The parametric study showed that the most important factor affecting the axial stiffness reduction factors is the amount of tension steel in the beam sections.

Beam section dimensions were also found to affect the value of the reduction factors. Analysis results indicated that the exaggerated value of the "uncracked axial stiffness" in case of beams of large sections, as compared to the actual "cracked axial stiffness" heightens the need for use of more accurate "Reduction factors"

in order to bring the finite element analysis assumptions closer to the practical case, where concrete cracking due to flexural behavior is significant.

A main recommendation is reached in this study regarding the value of the reduction factors used for the modification of the axial stiffness values of beam elements used in finite element analysis models. The use of a fixed reduction factor for all cases of temperature analysis is not appropriate. The values of the reduction factors to be used for analysis should be tied to the general percentage of steel rft in the beam sections. More accurate values for these reduction factors will definitely serve to simulate more accurately the expansion/contraction effect in RC structures, and can produce reduced (and more realistic) values of straining actions in the supporting columns.

References

[1]. ACI Committee 224.2R-92, Cracking of Concrete Members in Direct Tension, *ACI Structural Journal, 1992, pp. 6:7.*
[2]. ACI Committee 349.1R-07, Reinforced Concrete Design for Thermal Effects on Nuclear Power Plant Structures, *ACI Structural Journal, 2007, pp.4.*
[3]. ECP 203 (2017), Design & Construction of concrete structures, *HBRC Journal, 2017, pp. 6-22.*
[4]. Essam H. El-Tayeb, Salah E. El-Metwally, Hamed S. Askar, Ahmed M. Yousef, Thermal Analysis of Reinforced Concrete Beams and Frames, *HBRC Journal, 2015.*
[5]. Frank J. Vecchion, Nonlinear Analysis of Reinforced Concrete Frames Subjected to Thermal and Mechanical Loads, *ACI Structural Journal, 1987.*
[6]. Frank J. Vecchion, Agostinoa, N D B. Angelakos, Reinforced concrete slabs subjected to thermal loads, *Canadian Journal of Civil Engineering, Vol. 20, No. 5, pp. 741:753, 1993.*
[7]. Randy J. James, Ai-Shen Liu, Nonlinear Analyses for Thermal Cracking in the Design of Concrete Structures, *ICONE17, 2009*, San Jose, California, USA.

Hisham A. El-Arabaty. "Finite Element Modelling of Structures Subjected to Thermal Loading." IOSR Journal of Mechanical and Civil Engineering (IOSR-JMCE) , vol. 15, no. 6, 2018, pp. 31-43.